Numerical Investigation of Epidemics Transport Dynamics via a Coupled PDE Crowd Flow - Epidemics Spreading Dynamics Model ⋆

Anargiros I. Delis * **Nikolaos Bekiaris-Liberis** **

* *School of Production Engineering & Management, Technical University of Crete, 73100 Chania, Greece (e-mail: adelis@tuc.gr).*
** *School of Electrical and Computer Engineering, Technical University of Crete, 73100 Chania, Greece (e-mail: bekiaris-liberis@ece.tuc.gr)*

Abstract: We demonstrate the epidemics transport effect in closed spaces, performing different numerical experiments via development of a coupled, macroscopic partial differential equation (PDE) model of crowd flow, epidemics spreading dynamics, and ventilation air flow dynamics. We present numerical approximations for the coupled model with which we perform different numerical tests. In particular, we study the effect of different ventilation rates in epidemics transport (in time and space), also quantifying the infection risk via computing the total number of exposed individuals (in time and space), predicted by the model. We then discuss how the model used and the numerical results obtained could be utilized, in certain scenarios, for design of epidemics transport control strategies via manipulation of the ventilation air-flow field.

Keywords: Crowd flow dynamics, Epidemics transport, Macroscopic modeling, Numerical simulation

1. INTRODUCTION

The ramifications of epidemics spreading in economy Anderson et al. (2020) and physical/mental health Delmastro and Zamariola (2020), highlighted the need of accurate prediction of epidemics spreading. One way towards this is through modeling the dynamics of epidemics spreading. Due to the complexity of detailed description of epidemics spreading when accounting for individual-to-individual interactions, particularly when considering large spaces, or a high number of individuals, see, for example, Willem et al. (2017), macroscopic models may be utilized to describe epidemics spreading dynamics, see, for example, Vynnycky and White (2010). Even though such models capture epidemics spreading dynamics on a macroscopic scale, they may not capture the transporting behavior of epidemics, which is, in fact, the main, macroscopic phenomenon in epidemics spreading dynamics, emerging from people transport. Furthermore, one potential way of control of epidemics spreading in closed spaces is via manipulation of the ventilation rate, see, e.g., Hosseinloo et al. (2023), potentially accounting for the density (and speed) dynamics of people in time and space. For these two reasons, in the present paper, we perform numerical tests to study the epidemics transport dynamics, under the effect of various ventilation rates, utilizing a PDE model that accounts for crowd flow and epidemics spreading dynamics, as well as for the effect of ventilation rate.

In particular, we present a novel approach in which we utilize a PDE model consisting of three components; a component that describes crowd flow dynamics in a 2-D space, a component that describes epidemics spreading, essentially, being a macroscopic version of a (susceptible-exposed-infected-susceptible) SEIS-type model, and a component that describes the effect of aerosol dynamics to spreading, in particular, describing the effect of ventilation rate. The model we present here can be viewed as a modified version of the model considered in Salam et al. (2023), in that we use a relatively less complex crowd flow model (modified from Kachroo et al. (2008) to incorporate computation of the desired direction vector) and use potential theory to compute the ventilation induced air-flow field. Besides the model in Salam et al. (2023), papers Salam et al. (2021), Kim and Quaini (2020) also present relevant PDE models, consisting of a crowd flow dynamics component and an epidemics spreading component. Perhaps the main difference of the models in Salam et al. (2023), Kim and Quaini (2020) and in Salam et al. (2021) can be viewed as lying in that Salam et al. (2021), Kim and Quaini (2020) describe the effect of people movements/interactions to epidemics spreading in a more direct relation to microscopic considerations, essentially translating, in the macroscopic level, the effect of duration and distance of people contacts to epidemics spreading; whereas Salam et al. (2023) may be viewed as a higher level, macroscopic model, describing the effect of people density and ventilation rate to epidemics spreading. In fact, models Salam et al. (2021); Kim and Quaini (2020) can be useful more for design of epidemics spreading control strategies via manipulation of people trajectories, rather than via manipulation of the ventilation rate. Our work can be also viewed as relevant to papers that consider macroscopic models of coupled people/traffic flow and epidemics spreading dynamics, such as, e.g., Haghani (2022); Sattenspiel and Dietz (1995); Arino and Van den Driessche (2003); Tizzoni et al. (2014); Bertaglia and Pareschi (2021); Guan et al. (2020); Niazi et al. (2021). Although these works are relevant, they describe the coupled people flow - epidemics spreading process on a higher, macroscopic level (e.g., on the level of

⋆ Funded by the European Union (ERC, C-NORA, 101088147). Views and opinions expressed are however those of the authors only and do not necessarily reflect those of the European Union or the European Research Council Executive Agency. Neither the European Union nor the granting authority can be held responsible for them.

a country or a city), not considering the crowd movements in closed spaces, as we do here.

In the present paper, we perform numerical tests employing the proposed PDE model. In particular, we employ an accurate finite-volume-based numerical scheme to simultaneously solve on a 2-D domain the three components of the model, namely, the crowd flow, epidemics spreading, and aerosol dynamics models; while employing a finite-difference scheme for numerically solving a 2-D Laplace equation to obtain a simplified velocity field, corresponding to the operation of the ventilation system. Implementing these numerical schemes, we perform two main types of tests. In the first, we assume static conditions for the crowd and investigate epidemics spreading in space and time (within a closed space), for different ventilation rates. In the second, we account for people movements and potential exits, together with accounting for variable ventilation rates. We show that, as ventilation rate increases, the average density of exposed individuals, as predicted by the model, increases at a lower rate, also depending on the particular, ventilation-induced, air-flow field. In fact, our testings demonstrate epidemics transport dynamics in time and space, in the presence of ventilation. Thus, essentially, our results illustrate the possibility to utilize the density (and speed) profile in time/space in real time (i.e., to not only employing an average, total number of people), to manipulate ventilation air-flow field in closed spaces towards balancing epidemics spreading suppression and energy consumption.

2. COUPLED MODELING EQUATIONS

2.1 Crowd Flow Modeling

The model presented here is classified as nonlinear, hyperbolic PDE system (with source terms present). Second-order models in 2D use three, coupled PDEs to describe crowd flow; the mass conservation and two equations that resemble the momentum equations in fluid flow with a modification to the pressure term to mimic crowd motion. In essence, we consider pedestrians as a "thinking fluid". The model considered here is known for its isotropic nature, which is realistic assuming pedestrian motion is influenced from all directions. This model stems from the well-known Payne-Whitham (PW) traffic flow model Lighthill and Whitham (1955); Payne (1971), adapted to crowd flow dynamics Kachroo et al. (2008). We present the model in conservation law form, which eases the application of proper numerical methods (e.g., finite volume ones). In general, we consider a two-dimensional connected domain $\Omega \subset \mathbb{R}^2$ corresponding to some walking facility possibly equipped with some entrances or exits. The boundary of the domain $\partial\Omega = \Gamma_0 \cup \Gamma_w$ consists of outflow boundaries denoted by Γ_0 and walls Γ_w.

By denoting as $\mathbf{x} = (x, y) \in \Omega$ the spatial variables and $t > 0$ the time, we define as $\rho(x, y, t)$ the pedestrian density, that has to stay non-negative and bounded, i.e., $0 \le \rho(\mathbf{x}, t) \le \rho_{\max}$, while as $u(\mathbf{x}, t)$ and $v(\mathbf{x}, t)$ we define the $x-$component and $y-$component of the velocity vector $\mathbf{v}$, respectively. The model equations, and their initial conditions [1], can be written as (we refer, e.g., in Salam et al. (2023, 2021); Twarogowska et al. (2014))

$$\rho_t + \nabla \cdot (\rho \mathbf{v}) = 0, \tag{1}$$

$$(\rho \mathbf{v})_t + \nabla \cdot (\rho \mathbf{v} \otimes \mathbf{v} + P(\rho)) = \frac{1}{\tau}\rho\left(V(\rho)\boldsymbol{\mu} - \mathbf{v}\right), \tag{2}$$

$$\rho(\mathbf{x}, 0) = \rho_0(\mathbf{x}), \tag{3}$$

$$\mathbf{v}(\mathbf{x}, 0) = \mathbf{v}_0(\mathbf{x}), \tag{4}$$

where $P(\rho)$ is an internal pressure function. In the momentum equations (2) the relaxation source term drives $\mathbf{v}$ towards the desired speed $V(\rho)\boldsymbol{\mu}$, where $V(\rho)$ is an equilibrium speed-density relation, $\boldsymbol{\mu}$ is the desired direction vector, and τ is a relaxation time.

For the speed-density relation we implement the relation

$$V(\rho) = u_{\max} e^{-\alpha(\rho/\rho_{\max})^2}, \tag{5}$$

where $\alpha > 0$ is a constant, $u_{\max}$ is the free-flow velocity, and $V(\rho_{\max}) \approx 0$, with $\rho_{\max}$ being the congestion density at which the motion is hardly possible. We note here that other equilibrium speed-density relations can also be implemented. For the pressure function we choose $P(\rho) = \rho C_0^2$, with C_0^2 being a constant representing an anticipation factor.

For the desired direction of motion $\boldsymbol{\mu}$, and under the typical assumptions that pedestrians route choice is based on the shortest path to a destination and avoidance of high density regions, Hughes (2002); Twarogowska et al. (2014), we define a potential field Φ that describes the instantaneous travel cost to a destination with

$$\boldsymbol{\mu} = -\frac{\nabla\Phi}{\|\nabla\Phi\|}. \tag{6}$$

The potential $\Phi : \Omega \to \mathbb{R}$ is defined by the eikonal equation

$$\|\nabla\Phi\| = \frac{1}{V(\rho)}, \quad t > 0, \mathbf{x} \text{ in } \Omega, \tag{7}$$

$$\Phi = 0, \qquad \mathbf{x} \text{ in } \Gamma_o. \tag{8}$$

This choice for $\boldsymbol{\mu}$ implies that pedestrians have a knowledge of the density distribution in the whole domain at each time instant, and use this to estimate their travel time. Such a reaction might be triggered, for example, by a global view on the pedestrian crowd or by information supplied in real time by an agent dictating people trajectories.

Equations (1), (2) can be written in vector conservative form as

$$\mathbf{Q}_t + \mathbf{F}(\mathbf{Q})_x + \mathbf{G}(\mathbf{Q})_y = \mathbf{S}(\mathbf{Q}), \tag{9}$$

where $\mathbf{Q} = (\rho, \rho u, \rho v)^{\mathrm{T}}$ and the fluxes and sources given as

$$\mathbf{F}(\mathbf{Q}) = \begin{pmatrix} \rho u \\ \rho u^2 + \rho C_0^2 \\ \rho u v \end{pmatrix}, \mathbf{G}(\mathbf{Q}) = \begin{pmatrix} \rho v \\ \rho u v \\ \rho v^2 + \rho C_0^2 \end{pmatrix},$$

$$\mathbf{S} = \begin{pmatrix} 0 \\ \frac{1}{\tau}\rho\left(-V(\rho)\frac{\Phi_x}{\|\nabla\Phi\|} - u\right) \\ \frac{1}{\tau}\rho\left(-V(\rho)\frac{\Phi_y}{\|\nabla\Phi\|} - v\right) \end{pmatrix}. \tag{10}$$

The eigenvalues of the Jacobian matrices $\mathbf{A}(\mathbf{Q}) = \dfrac{\partial \mathbf{F}}{\partial \mathbf{Q}}$ and $\mathbf{B}(\mathbf{Q}) = \dfrac{\partial \mathbf{G}}{\partial \mathbf{Q}}$ are, respectively,

$$\lambda_1^A = u - C_0, \ \lambda_2^A = u, \ \lambda_3^A = u + C_0, \tag{11}$$

and

$$\lambda_1^B = v - C_0, \ \lambda_2^B = v, \ \lambda_3^B = v + C_0, \tag{12}$$

[1] Because boundary conditions vary, depending on the numerical test we implement, we present them in Sections III and IV. We note here that, well-posesness study of the complete model is beyond the scope of this work. Nevertheless, well-posesness can, in principle, be studied for certain initial and boundary conditions using, e.g., Bressan et al. (2011); Brezis (2011).

with their corresponding eigenvectors being linearly independent (i.e., the model is strictly hyperbolic) given as

$$\mathbf{e}^A_{1,3} = (1,\ u \pm C_0,\ v)^{\mathrm{T}}, \mathbf{e}^A_2 = (0,\ 0,\ 1)^{\mathrm{T}}, \tag{13}$$

and

$$\mathbf{e}^B_{1,3} = (1,\ u,\ v \pm C_0)^{\mathrm{T}}, \mathbf{e}^B_2 = (0,\ 1,\ 0)^{\mathrm{T}}. \tag{14}$$

System (9) preserves its isotropic nature, meaning that information from all directions affect pedestrians' motion. We provide here the eigenstructure of the system as it is employed in our numerical scheme in Section III.

2.2 Epidemic Spreading Model

The model utilized here is from Salam et al. (2023) and is based on a macroscopic version of a SEIS model where each type of pedestrian (SEI) moves with the crowd speed $\mathbf{v}$, resulting from the total crowd flow model (9). The density of each type of pedestrian satisfies then the following

$$\rho^S_t + \nabla \cdot (\rho^S \mathbf{v}) = \kappa\rho^I - \beta_I\rho^S, \tag{15}$$

$$\rho^E_t + \nabla \cdot (\rho^E \mathbf{v}) = \beta_I\rho^S - \theta\rho^E, \tag{16}$$

$$\rho^I_t + \nabla \cdot (\rho^I \mathbf{v}) = \theta\rho^E - \kappa\rho^I, \tag{17}$$

where ρ^S, ρ^E, and ρ^I are densities of the susceptible, exposed, and infected pedestrians, respectively, satisfying $\rho = \rho^S + \rho^E + \rho^I$. The model equations are supplied with relevant initial conditions ρ^S_0, ρ^E_0 and ρ^I_0, similarly to equations (1)–(4), satisfying $\rho_0 = \rho^S_0 + \rho^E_0 + \rho^S_0$. Further, β_I is the infection rate, κ is the recovery rate, and θ is the rate with which exposed persons are becoming infected. Pedestrians are potentially becoming exposed, when they are in contact with infected pedestrians. However, on the time scales under consideration, κ and θ are very small and set to zero in our numerical simulations, such that the number of infected pedestrians remains constant when there is no inflow of infected pedestrians.

We compute $\beta_I(\mathbf{x}, t) = i_0\beta(\mathbf{x}, t)$, where $\beta(\mathbf{x}, t)$ is the solution to the following drift-reaction-diffusion PDE in 2D, from Salam et al. (2023),

$$\beta_t + \nabla \cdot (\beta\mathbf{U}_G) = \nabla \cdot (\sigma\nabla\beta) - \nu\beta + \frac{\rho^I}{\rho}, \tag{18}$$

where $\beta(\mathbf{x}, 0) = 0$, $\mathbf{U}_G$ is a given velocity field of the surrounding air-flow in the domain, and σ is effective turbulent viscosity for the aerosols. The term $-\nu\beta$ models the fact that aerosol particles are settling due to the gravitational force Salam et al. (2023); Zhao et al. (2004). In this work we assume that σ is a constant equal to $1.2 \cdot 10^{-3}$ Zhao et al. (2004); Salam et al. (2023, 2021) and we get the velocity field of the surrounding air-flow using potential flow theory which will be described next. Parameter i_0 is determined by the infectivity (e.g., depending on biological/environmental factors or the types of closed spaces and ventilation systems considered) and is of $O(10^{-2})$ Salam et al. (2023, 2021).

In order to produce a steady velocity field $\mathbf{U}_G$ of the surrounding air-flow in the computational region Ω for model (18), it is assumed that the air flow is inviscid, incompressible, and irrotational Kaushik (2019). Thus, the produced steady flow is governed by Laplace's equation as

$$\Delta\Psi = 0, \tag{19}$$

where $\Psi(\mathbf{x})$ is the so-called velocity potential function. By implementing Neumann boundary conditions and imposing conditions on the derivative of the potential with respect to the normal direction, we introduce air-flows for inflow and outflow boundaries imitating in such a way the inflows from ventilation ducts and outflows from exhaust ducts. We then compute the velocity field $\mathbf{U}_G$ as

$$\mathbf{U}_G = \nabla\Psi. \tag{20}$$

.

3. NUMERICAL METHODS FOR THE MODEL

The main numerical approaches adopted here are based on the implementation of well-known conservative finite volume schemes to discretize model equations (9) for the crowd flow, equations (15)–(17) for the contagion model, and the advection part in equation (18) for the infection rate. Here we only give a brief presentation of them and we refer, for example, to the works in Leveque (2002) for more details in hyperbolic PDEs and their numerical solution, and in Kachroo et al. (2008) for crowd flow models in particular. To this end, the solution space (x, y, t) is split up into a uniform computational grid, where the grid spaces in the x and y directions are given by Δx and Δy, respectively, and in time direction by Δt. The positions of the ith and jth nodes in the x and y directions, and nth node in time direction (x_i, y_j, t^n), are given by $(i\Delta x, j\Delta y, n\Delta t)$ with the solution vector denoted as $\mathbf{Q}^n_{i,j}$ at the center of the computational cell $[x_{i-1/2,j}, x_{i+1/2,j}]\times[y_{i,j-1/2}, y_{i,j+1/2}]$. By doing so, the numerical schemes for 2D space can be written in a general finite volume form as

$$\mathbf{Q}^{n+1}_{i,j} = \mathbf{Q}^n_{i,j} - \frac{\Delta t}{\Delta x}\left[\mathbf{F}^n_{i+1/2,j} - \mathbf{F}^n_{i-1/2,j}\right] - \frac{\Delta t}{\Delta y}\left[\mathbf{G}^n_{i,j+1/2} - \mathbf{G}^n_{i,j-1/2}\right] + \Delta t\mathbf{S}^n_{i,j}, \tag{21}$$

where $\mathbf{F}^n_{i\pm1/2,j}$ and $\mathbf{G}^n_{i,j\pm1/2}$ are the numerical fluxes at the x and y (cell-boundary) directions, respectively.

For model equations (9) we implement the well-known approximate Riemann solver of Roe, Leveque (2002), to compute the numerical fluxes and we briefly describe it here. The idea behind Roe's scheme is to take a non-linear PDE system in quasi-linear form and linearize it locally by approximating the Jacobian matrices using the so-called Roe averages. Thus, for example, the numerical flux at the $(i + 1/2, j)$ interface of the ith computational cell is defined as

$$\mathbf{F}^{\mathrm{Roe}}_{i+1/2,j} = \frac{1}{2}\left[\mathbf{F}(\mathbf{Q}_{i+1,j}) + \mathbf{F}(\mathbf{Q}_{i,j})\right] - \frac{1}{2}\tilde{\mathbf{R}}|\tilde{\Lambda}|\tilde{\mathbf{R}}^{-1}[\mathbf{Q}_{i+1,j} - \mathbf{Q}_{i,j}], \tag{22}$$

using the fact that $|\mathbf{A}|(\tilde{\mathbf{Q}}) = \tilde{\mathbf{R}}|\tilde{\Lambda}|\tilde{\mathbf{R}}^{-1}$, where $\tilde{\mathbf{R}}$ is the (average) eigenvectors' matrix and $\tilde{\Lambda}$ is the diagonal matrix of the eigenvalues. For the crowd flow model, defining as $R \equiv (i + 1, j)$ and $L \equiv (i, j)$ the states on the right and left at the boundary intefrace, these averages are

$$\tilde{\rho} = \sqrt{\rho_R \cdot \rho_L}, \tilde{u} = \frac{u_L\sqrt{\rho_L} + u_R\sqrt{\rho_R}}{\sqrt{\rho_R} + \sqrt{\rho_L}}, \tilde{v} = \frac{v_L\sqrt{\rho_L} + v_R\sqrt{\rho_R}}{\sqrt{\rho_R} + \sqrt{\rho_L}}, \tag{23}$$

which are used to compute $\tilde{\mathbf{R}}$ and $\tilde{\Lambda}$, according to (11)–(14). The same procedure is performed for $\mathbf{G}^n_{i,j+1/2}$ along y direction. This scheme is stable under the usual Courant-Friedrichs-Lewy (CFL) stability condition Leveque (2002, 2007).

For the boundary conditions, we implement the following, at a layer of grid points (ghost cells) around the computational domain.

- Free-slip at walls: $\rho_g = \rho_i$, $\mathbf{v}_g = \mathbf{v}_i - 2(\mathbf{v}_i \cdot \mathbf{n})\mathbf{n}$, with i being the neighbor point inside the domain and $\mathbf{n}$ the unit normal vector at a boundary cell.
- Outflow (at exits): $\rho_g = \rho_i$, $\mathbf{v}_g = u_{\max}\mathbf{n}$ (assuming on exits pedestrians can leave with maximum speed).

Finally, for the crowd flow model, and to numerically obtain the direction vector $\boldsymbol{\mu}$ in the relaxation source term, we numerically solve the eikonal equation (7), (8) at each time step implementing the Fast-Sweeping Method (FSM) of Zhao (2005).

For model equations (15)–(17) for the contagion model and the advection part in equation (18) we implement the well-known Rusanov flux in scheme (21), which reads, for example, in the x direction as

$$\mathbf{F}^{\text{Rus}}_{i+1/2,j} = \frac{1}{2}\left[\bar{\mathbf{F}}(\mathbf{Q}_{i+1,j}) + \bar{\mathbf{F}}(\mathbf{Q}_{i,j})\right] - \frac{C_{i+1/2,j}}{2}[\mathbf{Q}_{i+1,j} - \mathbf{Q}_{i,j}], \quad (24)$$

where $C_{i+1/2,j} = \max\{|u_{i,j}|, |u_{i+1,j}|\}$, i.e., is the maximum absolute velocity in the x direction, and similar is the formulation in the y direction and the numerical flux $\mathbf{G}^{\text{Rus}}$. Here $\bar{\mathbf{F}}$ and $\bar{\mathbf{G}}$ are the advection fluxes in (15)–(17) and (18).

Further, for the diffusion term $\nabla \cdot (\sigma \nabla \beta)$ in equation (18), as well as, for solving the Laplace equation (19) classical, second-order central finite-differences scheme are implemented Leveque (2007) with Neumann boundary conditions.

4. NUMERICAL TESTS AND RESULTS

In this section we present numerical simulations for evaluating the behavior of the model and, in particular, for evaluating the effect of variable ventilation rate on epidemic spreading. If not otherwise stated, the parameters used in all the simulation scenarios presented below are $\rho_{\max} = 6$ ped/m^2, $u_{\max} = 2m/s$, $\tau = 0.6s$, $\alpha = 7.5$ for the density-speed coefficient of $V(\rho)$, $C_0 = 0.8$ for the anticipation factor, and $i_0 = 0.04$ (as in Salam et al. (2023, 2021)) for the infectivity rate.

4.1 Crowd at Rest

In this test we consider a closed room of size $\Omega = [0, 10m] \times [0, 10m]$. In this situation the crowd in the room is stationary (no movement is taking place) and we implement wall boundary conditions in all model equations. Further, we assume one inflow ventilation duct at the middle of the left boundary and one exhaust duct at the middle of the right boundary, both being $1m$ wide. To produce the steady velocity field $\mathbf{U}_G$ from (19), (20), the derivative of the potential Ψ normal to the ventilation boundaries was set equal to $\mathbf{u}_{in} = (u_{in}, 0)$ for the left boundary and $\mathbf{u}_{out} = (-u_{in}, 0)$ for the right boundary, as to introduce the air-flow in the computational domain. In Fig. 1 we show the obtained velocity and the corresponding streamlines using $u_{in} = 5m/s$ for $\Delta x = \Delta y = 0.1m$ and $\Delta t = 0.02s$.

In these preliminary tests we aim to investigate the effect to the spread of a contagion in the room, via β_I, based on different values of the air supply velocities u_{in} and u_{out}, and various values of ν in (18). Both of these types of parameters are related to the effect of the aerosol dynamics. We first assume that the crowd density is $\rho_0(\mathbf{x}) = 1$ped/m^2 leading to 100 people being in the room and $\mathbf{v}_0 = 0$ in the crowd flow model. Further, we assume that 5% of the people are infected, uniformly spread in the room, i.e., $\rho_0^I = 0.05\rho_0$, leaving 95 people initially susceptible, i.e., $\rho_0^S = 0.95\rho_0$, while initially $\rho_0^E = 0$. We study the effect of using first $u_{in} = 5m/s$ with $\nu = 0.1$ and $\nu = 0.4$.

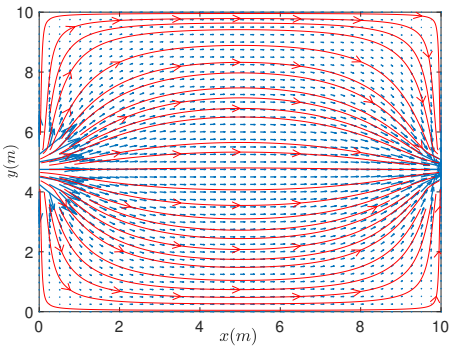

Fig. 1. Velocity field $\mathbf{U}_G$ vectors (in blue) and the corresponding streamlines for a ventilated room with a crowd at rest.

Then we perform the same simulation increasing the ventilation speed to $u_{in} = 10m/s$. An example of the obtained distribution of the exposed pedestrians at time $t = 300s$ is shown in Fig. 2, where we can see that the spreading follows the path of the induced airflow with higher concentrations on the outflow ventilation boundary. Next, in Fig. 3 we provide the evolution in time of the exposed pedestrians. We compute this total number inside the domain via relation $E(t) = \int_\Omega \rho^E(\mathbf{x}, t)d\mathbf{x}$. It is

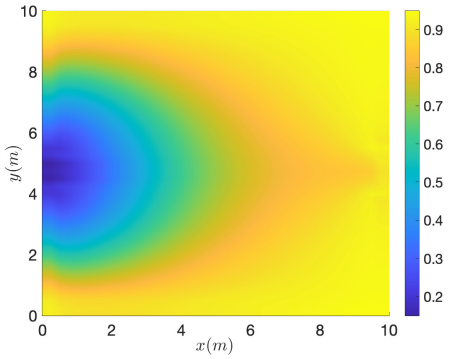

Fig. 2. Crowd at rest: Density of exposed pedestrians, ρ^E, at $t = 300s$, for $\rho_0(\mathbf{x}) = 1$ped/m^2, $\rho_0^I = 0.05\rho_0$, using $\nu = 0.1$ and $u_{in} = 5m/s$.

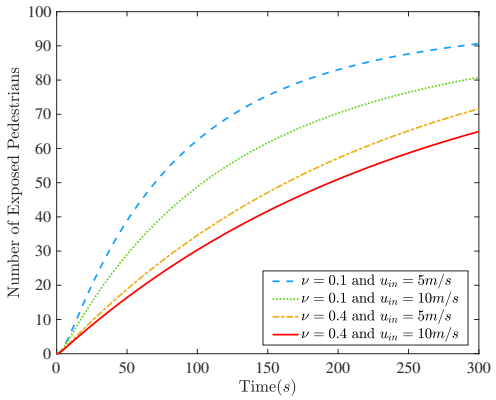

Fig. 3. Crowd at rest: Time evolution of predicted exposed pedestrians, for $\rho_0(\mathbf{x}) = 1$ped/m^2 and $\rho_0^I = 0.05\rho_0$.

evident form Fig. 3 that for both values of ν, increasing the ventilation air speed in the room substantially lowers the rate at which people are exposed. As expected, assuming a higher value for ν (which depends on the size of aerosol particles)

again decreases the number of exposed persons in the room (as smaller particles stay longer in the air). Furthermore, we observe that the higher the ventilation rate the slower the spreading, which is reasonably expected (see, e.g., Qian and Zheng (2018); Lipinski et al. (2020)). These results indicate that one can control the inflow/outflow air speed in the ventilation ducts to reduce the rate of increase of exposed persons, based on, e.g., real-time measurements of ρ in time/space.

4.2 Crowd Flow Towards an Exit

We consider a walking facility of size $\Omega = [0, 50m] \times [0, 20m]$ with an exit $6m$ wide at the right boundary centered at $y = 10m$. The initial density is $\rho_0(\mathbf{x}) = 1\text{ped}/m^2$ in the region $[0, 20m] \times [0, 20m]$, leading to 400 people in this region, with $\mathbf{v}_0(\mathbf{x}) = 0$ in the crowd flow model. Further, $\rho_0^I = 0.05\rho_0$, while initially $\rho_0^E = 0$. We perform three simulations in this test, where for the first one we assume that there is no ventilation imposed in the facility and in the next two we employ the velocity field $\mathbf{U_G}$, as shown in Fig. 4, imposing two inflow ventilation ducts at the middle of the top and bottom boundaries and two exhaust ducts at the middle of the right and left boundaries, all being $8m$ wide. We consider two cases for the ventilation speed, one with $u_{in} = 5m/s$, $u_{out} = -5m/s$, and one with $u_{in} = 10m/s$, $u_{out} = -10m/s$. In all tests here we fix the value of ν to 0.5.

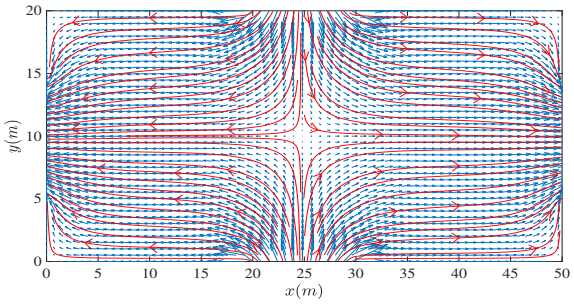

Fig. 4. Velocity field $\mathbf{U}_G$ vectors (in blue) and the corresponding streamlines (in red) for the moving crowd for $u_{in} = 10m/s$.

In Figs. 5 and 6 we show two time instances (for $t = 15s$ and $t = 25s$) of the evolution of total crowd density ρ, infection coefficient β_I, and density of exposed pedestrians ρ^E, inside the walking domain, when $u_{in} = 10m/s$. As it can be seen, the pedestrians move towards the exit at the right boundary and by time $t = 25s$ a clogging situation has been formed, where pedestrians accumulate around the exit. The evolution of the infection coefficient in the domain is clearly affected by the induced ventilation air field. At around $t = 40s$ all pedestrians have exited the domain. We note that, at an outflow boundary (exit) we keep track of the amount of exposed pedestrian that have been exited the domain. Thus, in Fig. 7 we show the evolution of the total number of exposed pedestrians in time for the three simulations performed. It is evident that increasing the ventilation air speed in the room substantially lowers the rate at which people are exposed, as well as the total number of exposed pedestrians. As expected, after exiting the domain the total number of exposed pedestrians remains constant.

We also observe that the type of the air flow field created by a given ventilation system also affects epidemics spreading rate and magnitude. In particular, we observed in our simulations (due to space limitation are not presented here) that when the air flow field is as in Fig. 4, then, in general, spreading is reduced

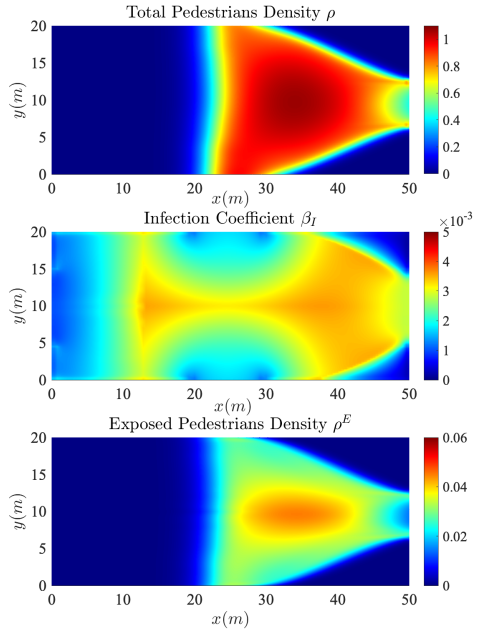

Fig. 5. Crowd flow towards an exit: Evolution of ρ, β_I, and ρ^E at $t = 15s$.

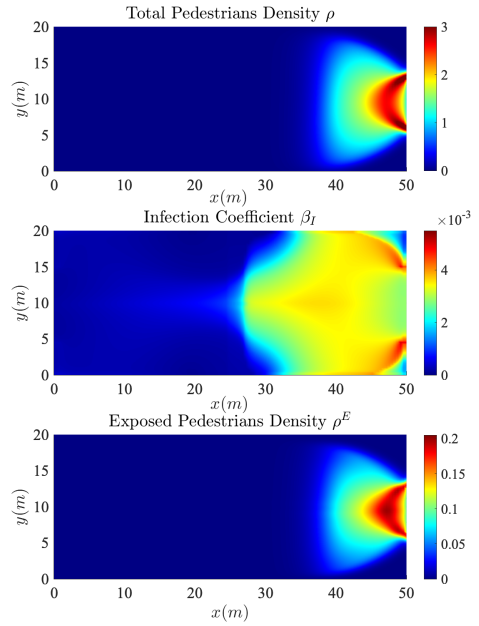

Fig. 6. Crowd flow towards an exit: Evolution of ρ, β_I, and ρ^E at $t = 25s$.

both in magnitude and rate, as compared with a system creating the field as in Fig. 1, for similar behavior of people movement in terms of speed, density, and direction. These observations may be useful for design of a ventilation system, potentially depending on a specific direction of people movement. The observed spreading dynamics' dependence on direction of air flow field is consistent with, e.g., Qian and Zheng (2018); Lipinski et al. (2020).

5. CONCLUSIONS AND CURRENT WORK

We presented numerical investigations implementing a PDE model consisting of a coupled crowd flow - epidemics spread-

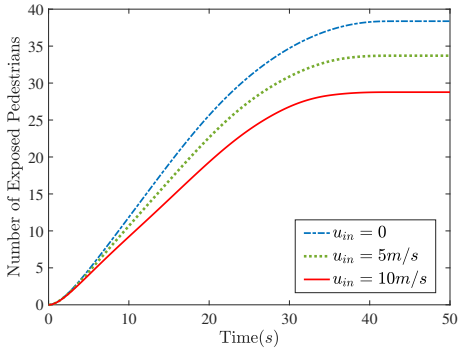

Fig. 7. Crowd flow towards an exit: Time evolution of predicted exposed pedestrians, for different ventilation rates.

ing process. We studied the effect of ventilation air flow profile to epidemics spreading accounting for people movements in closed spaces. We observed that higher ventilation rates, in general, reduce epidemics spreading. However, such a relation also depends on the specific people movement direction and speed, as well as on the specific air flow field. We are currently performing additional tests for various initial/boundary conditions of people density/speed, various directions of movement at different free flow velocities, and different ventilation air flow fields/magnitudes to validate further our findings. Further, we are also currently investigating the effect of incorporating vaccinated/masked individuals in the model equations, which may act, as alternative, epidemic transport control measure.

REFERENCES

Anderson, R.M., Heesterbeek, H., Klinkenberg, D., and Hollingsworth, T.D. (2020). How will country-based mitigation measures influence the course of the covid-19 epidemic? *Lancet*, 395, 931–934.

Arino, J. and Van den Driessche, P. (2003). A multi-city epidemic model. *Math. Population Studies*, 10, 175–193.

Bertaglia, G. and Pareschi, L. (2021). Hyperbolic models for the spread of epidemics on networks: Kinetic description and numerical methods. *ESAIM Math. Model. & Numerical Analysis*, 55, 381–407.

Bressan, A., Chen, G.Q.G., Lewicka, M., and Wang, D. (eds.) (2011). *Nonlinear Conservation Laws and Applications*. Springer, New York.

Brezis, H. (2011). *Functional Analysis Sobolev Spaces and Partial Differential Equations*. Springer, New York.

Delmastro, M. and Zamariola, G. (2020). Depressive symptoms in response to covid-19 and lockdown: a cross-sectional study on the italian population. *Nature Scientific Reports*, 10. Article no 22457.

Guan, L., Prieur, C., Zhang, L., Prieur, C., Georges, D., and Bellemain, P. (2020). Transport effect of covid-19 pandemic in france. *Annual Reviews in Control*, 50, 394–408.

Haghani, M. (2022). Crowd dynamics research in the era of covid-19 pandemic: Challenges and opportunities. *Safety Science*, 153. Paper no. 105818.

Hosseinloo, A., Nabi, S., Hosoi, A., and Dahleh, M. (2023). Data-driven control of covid-19 in buildings: a reinforcement-learning approach. *IEEE Trans. on Automation Science and Engineering*.

Hughes, R.L. (2002). A continuum theory for the flow of pedestrians. *Transp. Res. Part B: Method.*, 36(6), 507–535.

Kachroo, P., Wadoo, S., Al-nasur, S.J., and Shende, A. (2008). *Pedestrian Dynamics: Feedback Control of Crowd Evacuation*. Springer, Berlin.

Kaushik, M. (2019). Potential flow theory. In *Theoretical and Experimental Aerodynamics*. Springer, Singapore.

Kim, D. and Quaini, A. (2020). Coupling kinetic theory approaches for pedestrian dynamics and disease contagion in a confined environment. *Math. Models and Meth. in Applied Sciences*, 30, 1893–1915.

Leveque, R.J. (2002). *Finite Volume Methods for Hyperbolic Problems*. Cambridge University Press, U.K.

Leveque, R.J. (2007). *Finite Difference Methods for Ordinary and Partial Differential Equations: Steady-State and Time-Dependent Problems*. SIAM, Philadelphia.

Lighthill, M.J. and Whitham, G. (1955). On kinematic waves, *i*:flow movement in long rivers. *ii*:a theory of traffic on long crowded roods. *Proc. Royal Soc. A*, A229, 281–316.

Lipinski, T., Ahmad, D., Serey, N., and Jouhara, H. (2020). Review of ventilation strategies to reduce the risk of disease transmission in high occupancy buildings. *International Journal of Thermofluids*, 7-8.

Niazi, M., Canudas-de-Wit, C., Kibangou, A., and Bliman, P.A. (2021). Optimal control of urban human mobility for epidemic mitigation. In *2021 60th IEEE Conference on Decision and Control (CDC)*, 6958–6963. TX, USA.

Payne, H.J. (1971). Models of freeway traffic and control. *Math. Models Publ. Sys. Simul. Council Proc.*, 28, 51–61.

Qian, H. and Zheng, X. (2018). Ventilation control for airborne transmission of human exhaled bio-aerosols in buildings. *Journal of Thoracic Disease*, 10, S2295–S2304.

Salam, P.S.A., Bock, W., Klar, A., and Tiwari, S. (2021). Disease contagion models coupled to crowd motion and mesh-free simulation. *Math. Models and Meth. in Applied Sciences*, 31, 1277–1295.

Salam, P.S.A., Bock, W., Klar, A., and Tiwari, S. (2023). Coupling pedestrian flow and disease contagion models. In N. Bellomo and L. Gibelli (eds.), *Crowd Dynamics, Volume 4: Analytics and Human Factors in Crowd Modeling*, 223–246. Springer International Publishing, Cham.

Sattenspiel, L. and Dietz, K. (1995). A structured epidemic model incorporating geographic mobility among regions. *Mathematical Biosciences*, 128, 71–91.

Tizzoni, M., Bajardi, P., Decuyper, A., Kon Kam King, G., Schneider, C.M., Blondel, V., Smoreda, Z., Gonzalez, M.C., and Colizza, V. (2014). On the use of human mobility proxies for modeling epidemics. *Plos Computational Biology*, 10. Article number e1003716.

Twarogowska, M., Goatin, P., and Duvigneau, R. (2014). Macroscopic modeling and simulations of room evacuation. *Applied Mathematical Modelling*, 38(24), 5781–5795.

Vynnycky, E. and White, R. (2010). *An Introduction to Infectious Disease Modelling*. Oxford Univ. Press.

Willem, L., Verelst, F., Bilcke, J., Hens, N., and Beutels, P. (2017). Lessons from a decade of individual-based models for infectious disease transmission: a systematic review (2006-2015). *BMC Infectious Diseases*, 17. Paper no. 612.

Zhao, B., Zhang, Z., Li, X., and Huang, D. (2004). Comparison of diffusion characteristics of aerosol particles in different ventilated rooms by numerical method. In *ASHRAE Transactions*, volume 110 PART 1, 88 – 95.

Zhao, H. (2005). A fast sweeping method for eikonal equations. *Mathematics of Computation*, 74(250), 603–627.